Defect and Diffusion Forum
ISSN: 1662-9507, Vol. 450, pp 71-81
doi:10.4028/p-wko6TW

Submitted: 2026-01-16
Revised: 2026-02-15
Accepted: 2026-02-22
Online: 2026-04-15

Scaling Methodology for Large Boring Bars with Tuned Mass Dampers

Mikel Etxebeste[1,a*], Iñaki M. Arrieta[1,b], Gorka Ortiz-de-Zarate[1,c] and Pedro J. Arrazola[1,d]

[1]Mondragon Unibertsitatea, Faculty of Engineering, Loramendi 4, Arrasate-Mondragón, 20500, Spain

[a*]metxebeste@mondragon.edu, [b]imarrieta@mondragon.edu, [c]gortizdezarate@mondragon.edu, [d]pjarrazola@mondragon.edu

*corresponding author

Keywords: machining, boring, tuned mass damper (TMD), FEM, chatter, modeling.

Abstract. Sectors such as energy, aerospace, and heavy machinery increasingly rely on the machining of large components, where boring bars can easily exceed 200 mm in diameter and reach length-to-diameter ratios of up to 14. In these operations, chatter remains the dominant limitation due to the inherently low dynamic stiffness of such long tools. While Tuned Mass Dampers (TMDs) are widely applied in small and medium-sized boring bars, but transferring this technology to large-scale tools introduces significant challenges, particularly in the selection and tuning of damper components and the difficulty of evaluating performance prior to manufacturing. Because producing large boring bars is costly, a structured and predictive design strategy is essential to avoid trial-and-error iterations. This work introduces a scaling methodology that adapts TMD-integrated boring bar designs to large dimensions, providing a systematic approach to predict dynamic behavior across different tool sizes. The methodology is demonstrated through a case study involving Ø200 mm boring bar with length of 14 times the diameter. Experimental validation with the manufactured prototype confirms that the proposed scaling strategy enables effective chatter suppression and offers a practical path for extending TMD technology to large-scale boring applications.

1. Introduction

Industrial sectors such as energy, aerospace, and heavy machinery increasingly demand larger and more complex components to improve performance and reliability. Internal turning of these parts often requires boring bars with long overhangs, where geometric accuracy and surface quality depend heavily on the tool's dynamic behavior [1]. As tool dimensions scale with component size, the inherent reduction in stiffness makes the boring bar the main limitation in machining performance, particularly due to its susceptibility to chatter [2]. Ensuring effective vibration suppression in large boring bars is therefore essential for maintaining productivity and process robustness.

Chatter remains a dominant constraint in deep boring operations [3]. It arises from the regenerative effect between tool passes, creating self-excited vibrations that degrade surface finish, reduce dimensional precision, and limit material removal rates [4,5]. Long and slender boring bars are especially vulnerable because increasing overhang reduces stiffness and natural frequencies, making the tool highly sensitive to cutting-force excitation [6]. For large boring bars, the significant mass further amplifies compliance, creating additional challenges for achieving both rigidity and manageable tool weight [7]. Stability Lobe Diagrams (SLDs) have been widely used to identify stable cutting regimes [6,8], yet modifying cutting conditions alone is rarely sufficient in large-scale internal turning, reinforcing the need for enhanced tool designs.

Numerous passive, semi-active, and active vibration suppression strategies have been explored, including Tuned Mass Dampers (TMDs) [9–12], magnetorheological systems [13–16], piezoelectric actuators [17–19], electromagnetic solutions [20–22], topology-optimized structures [23–25], and high-damping materials [26–28]. Among these, passive strategies are generally favored for industrial implementation due to their simplicity and reliability. TMDs are particularly prominent in boring applications [5,31]. They introduce a secondary mass–spring–damper subsystem tuned to the

dominant mode of the bar, and when properly adjusted, the TMD attenuates the resonance peak and increases dynamic stability [4,5]. Variants such as friction dampers [32], impact absorbers [33], Lanchester systems [34,35], and eddy-current dampers [36,37] have also been investigated, but TMDs remain the preferred solution for industrial use because of their robustness and straightforward integration [38]. Commercial TMD bars perform well for smaller diameters and overhangs up to $L = 10\times Ø$ [38], but scaling this technology to very large boring bars introduces challenges that current literature only partially addresses.

When tool dimensions exceed conventional ranges, directly scaling TMD solutions from smaller bars becomes ineffective. At large scales, the dynamic response is dominated by mass distribution, internal architecture, and limitations in achievable tuning frequencies. Empirical prototyping is costly and often impractical, making predictive scaling strategies essential. Analytical models remain common in boring bar design [3,8], but they offer limited fidelity for representing complex internal layouts or supporting iterative optimization. Finite Element Method (FEM) approaches, by contrast, have proven effective for designing TMD-equipped tools and predicting chatter behavior [39,40]. Although FEM has been applied to small TMD boring bars [40], composite designs [41], and stability boundary estimation [42], the literature still lacks an integrated framework for large-scale tools. To date, no existing approach offers a unified and efficient methodology for the design of large boring bars equipped with TMDs.

This review highlights that despite extensive work on chatter suppression and TMD technologies, a consolidated scaling approach suitable for very large boring bars, particularly those exceeding $14\times Ø$, has not been documented. The high manufacturing cost and demanding performance requirements of such tools make the absence of systematic design strategies especially problematic, as trial-and-error manufacturing cycles are unrealistic in industrial environments.

To address these gaps, this work presents a scaling methodology for large boring bars incorporating TMD. The approach provides a structured framework to extrapolate TMD concepts to larger dimensions and guide the design of scalable configurations. The methodology includes the analysis of boring bar and TMD scaling relations, TMD design and tuning for large-scale applications, and experimental validation. A case study involving Ø200 mm bar with $14\times Ø$ overhang is used to demonstrate the approach, including prototype manufacturing and testing. Results show that the proposed scaling methodology offers an effective path for extending TMD technology to large boring bars, enabling stable machining performance across tool sizes.

2. Methodology

The proposed scaling methodology provides a structured framework for designing large boring bars equipped with TMDs. It integrates the analysis of dynamic behavior across varying bar diameters and lengths with TMD configuration, enabling standardized procedures for future tool development while minimizing modeling and validation efforts. Analytical models are employed to efficiently predict dynamic responses and extract modal parameters necessary for TMD tuning. The methodology also introduces a TMD design suitable for large boring bars and adaptable to different tool geometries. Overall workflow, consists of four main steps (Figure 1):

(i) Case study definition: Each boring bar is defined by its diameter (Ø), overhang length (L), and key design characteristics relevant to scaling and TMD integration. This step establishes the baseline configuration for the subsequent analyses and design procedures.

(ii) Boring bar scaling analysis: Analytical formulations are applied to assess bar stiffness and natural frequencies across different diameters and lengths. The methodology focuses primarily on bars with lengths around $L = 14\times Ø$ and diameters between 100 mm and 500 mm. Slenderness is evaluated to determine whether the geometry can be reliably scaled from previous analyses, while TMD requirements are concurrently considered to ensure proper integration.

(iii) TMD design and tuning: Based on the predicted modal parameters from the scaling analysis, the TMD is designed and tuned. Flexible couplings are characterized, and the TMD mass is calculated to maximize vibration suppression according to the selected tuning criteria. The

dynamic Frequency Response Function (FRF) of the boring bar, both with and without the TMD, are compared to verify effectiveness and confirm the design's ability to mitigate chatter.

(iv) Experimental validation: The final step involves experimental verification of the methodology and the designed boring bars. Experimental Modal Analysis (EMA) through tap-testing is conducted to characterize the dynamic behavior at various overhang lengths, confirming that the scaling methodology and TMD design achieve the intended vibration control.

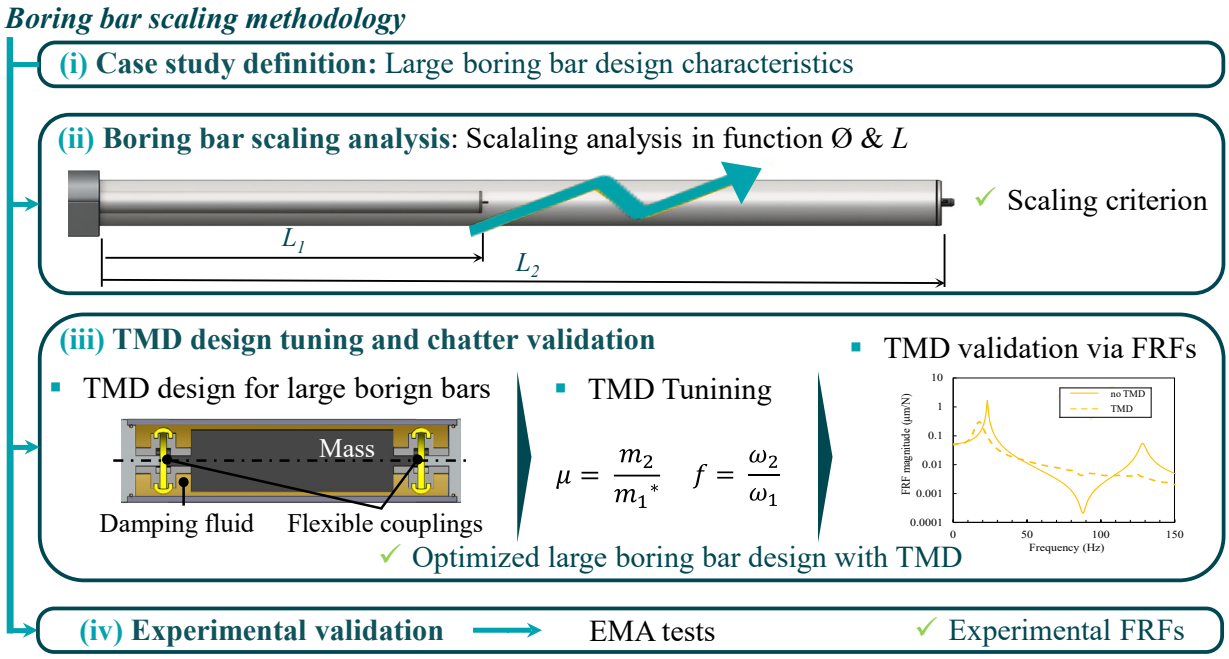

Fig. 1. Scaling methodology for optimized large boring bars with TMD and its experimental validation.

2.1. Case Study Definition

The scaling methodology was developed and validated through a real case study involving a boring bar with a length-to-diameter ratio of $L = 14\times Ø$, a diameter of Ø200 mm, and an overhang length of $L = 2800$ mm. The analysis was conducted at this constant ratio to isolate tool diameter as the primary scaling variable, since diameter and length effects do not scale linearly in large boring bars. Scaling analysis and dynamic evaluation were performed for both tool configurations to assess feasibility and dynamic performance.

The study focused on the critical bending mode of the boring bars, as torsional and axial responses were found to have a negligible influence. Figure 2 shows representative designs of the case study bar, highlighting the main cylindrical bar, the end caps, the tool-holder with cutting insert, and the integrated TMD assembly.

The employed clamping system was a double-clamping configuration, which is commonly used for large boring bars. The first clamp is wider (a) and the second narrower (b), with an adjustable spacing (λ) between them. In industrial practice, the same clamping fixture can be reused for different bar diameters by employing sleeves, ensuring flexibility across tool sizes.

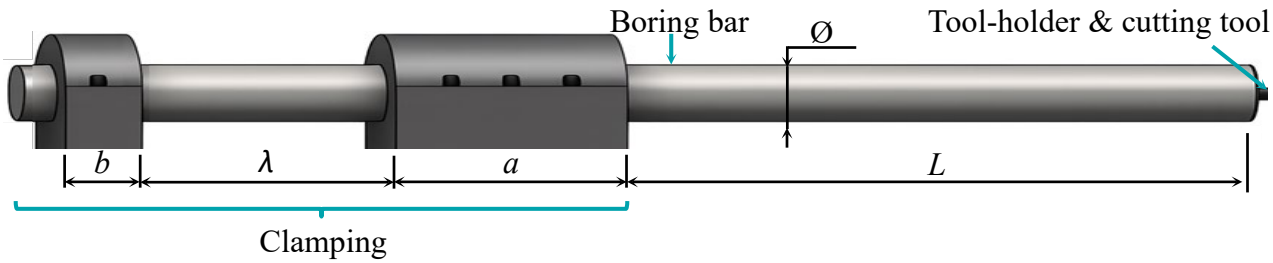

Fig. 2. Case study boring bar definition.

Key parameters for the boring bars, including geometric dimensions, material properties, and clamping dimensions, are summarized in Table 1. These parameters provide the basis for scaling analysis, predicting dynamic behavior and guiding the TMD design and tuning process.

Table 1. Case study definition and material properties.

Parameter	Value
Boring bar:	
Ø (mm)	200
L (mm) 14×Ø	2800
Clamping	
a (mm)	620
b (mm)	100
λ (mm)	1200
Material properties:	
Density, ρ (kg/m^3)	7800
Young's modulus, E (GPa)	210
Poisson's ratio, ν (-)	0.28

2.2. Scaling Analysis

The scaling analysis of the defined boring bars was performed using analytical formulations to evaluate stiffness (k) and natural frequency (ω_n) as functions of diameter (Ø) and length (L). Both bars were modeled as Euler–Bernoulli cantilever beams with a constant circular cross-section (Equations (1)-(2)), neglecting additional structural features such as tool-holder or end caps. Material properties are reported in Table 1.

$$k = \frac{F}{\delta} = \frac{3 \cdot E \cdot I}{L^3} = \frac{3 \cdot E \cdot \pi \cdot Ø^4}{L^3 \cdot 64} \tag{1}$$

$$\omega_n = \sqrt{\frac{k}{m_{eff}}} = \sqrt{\frac{E \cdot Ø^2}{\rho \cdot 16}} \cdot \frac{1}{2\pi} \cdot \left(\frac{k_i}{L}\right)^2 \tag{2}$$

where δ is the tool-tip deflection under an applied force F, E is the Young's modulus of the bar, I is the moment of inertia, ρ is the material density, m_{eff} represents the fraction of the bar's mass actively participating in the vibration mode, and k_i is a mode-dependent factor (for the first bending mode, k_i = 1.875).

A sensitivity analysis was conducted to evaluate how variations in diameter and length affect stiffness and natural frequency. This analysis provides a systematic framework to predict performance trends and assess the scalability of boring bars, both for tools sharing the same length-to-diameter ratio and for tools with different geometric proportions. The results offer practical guidance for extending TMD design and tuning strategies across a wide range of industrial boring bar configurations.

2.3. Scalable TMD Design

A specific TMD was developed for the large boring bars in the case study. The TMD is positioned near the tool tip and consists of a mass supported by flexible couplings, fully immersed in damping fluid. Its dynamic behavior is modeled as a secondary mass connected to the bar through a spring (k_2) and a damper (c_2) (Figure 3). The complete assembly includes an external sleeve and end caps sealed with O-rings. When the bar vibrates, the flexible couplings allow the TMD mass to oscillate out of phase, dissipating energy through polymer coupling elasticity and viscous damping in the fluid.

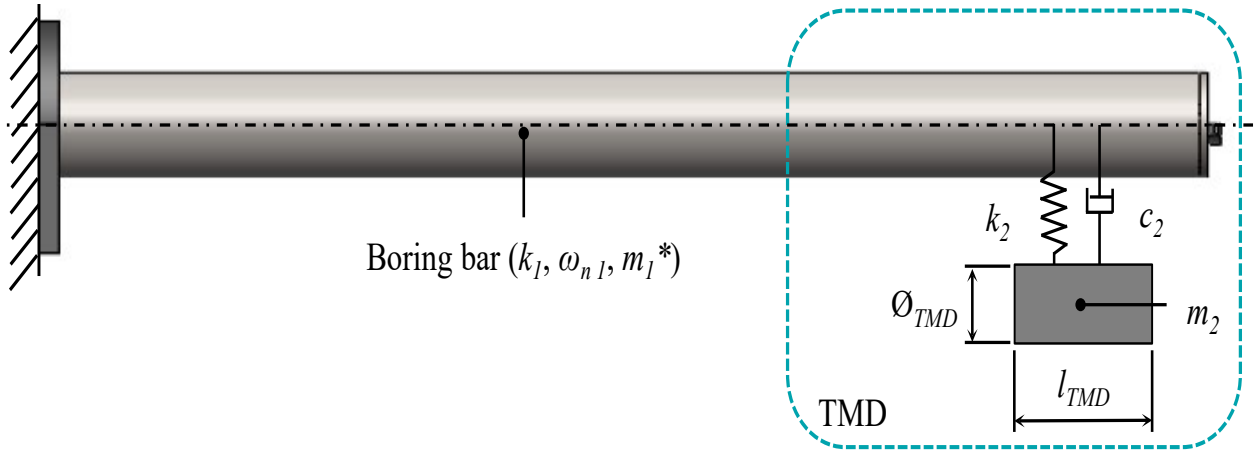

Fig. 3. TMD design for large boring bars and dynamic model.

The TMD is tuned to the primary bending mode of each bar. The tuning process considers: (i) modal parameters of the bar (stiffness k_1, natural frequency ω_1, and effective modal mass m_1*), (ii) stiffness of the flexible couplings (k_2), which sets the required TMD mass (m_2), and (iii) geometric and material constraints for the TMD. Optimal tuning is achieved when the TMD natural frequency (ω_2) matches the bar's target frequency (ω_1), producing a counteracting inertial force that reduces the tool-tip vibration peak and enhances dynamic stability. The effective TMD mass is determined by Equations (3). Once defined, the mass ratio (μ) can be achieved to assess the tuning by Equations (3). The corresponding damping coefficient (c_2) for TMD simulation and validation was obtained using Equation (5), where (ζ) is the damping ratio.

$$f = \frac{\omega_2}{\omega_1} \rightarrow \text{for } f = 1: \; m_2 = \frac{k_2}{{\omega_1}^2} \tag{3}$$

$$\mu = \frac{m_2}{{m_1}^*} \tag{4}$$

$$c_2 = 2\,\zeta\,\sqrt{k_2\,m_2} \tag{5}$$

where μ is the mass ratio being around 20% for enhanced vibration attenuation. The TMD mass geometry (diameter $Ø_{TMD}$, length L_{TMD}) and material are iteratively selected to satisfy the required mass and fit within the available housing.

Dynamic performance is validated using FRFs computed with a substructure approach, which couples the bar's receptance with the TMD dynamics based on the model in Figure 3a. The design is confirmed when the initial vibration peak of the boring bar is effectively attenuated by the TMD. This approach also allows iterative sensitivity analyses of the TMD configuration and component selection, providing a reliable prediction of vibration reduction at the primary bending mode.

2.4. Experimental Validation Procedure

The proposed methodology was validated through prototype manufacturing and experimental testing. The bar was mounted in a Geminis L CNC lathe (maximum diameter 2 m and length of 10 m) using the described clamping configuration. EMA was conducted using tap-testing: the bar was excited with an impact hammer (Brüel & Kjaer Type 8206), and dynamic responses were recorded with an accelerometer (Brüel & Kjaer Type 4525-B) (Figure 4).

The TMD-integrated boring bar was tested at multiple effective lengths (L'), starting from the target overhang of 14×Ø (2800 mm) and sequentially reduced in 500 mm increments, resulting in four test configurations (L' = 2800, 2300, 1800, 1300). Measured FRFs were analyzed to assess TMD effectiveness across different lengths and to validate the predictive models by comparing experimental and simulated responses.

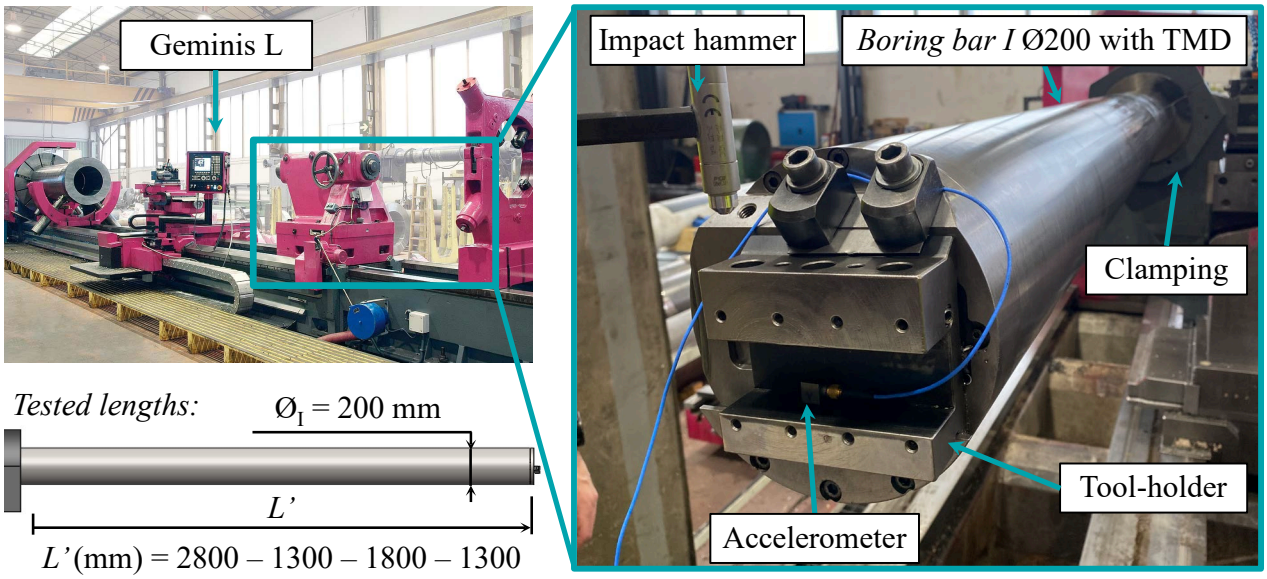

Fig. 4. EMA of Ø200 boring bar.

3. Results and Discussion

The results obtained from the scaling methodology, TMD design and tuning, and the experimental validation were analyzed and discussed.

3.1. Scaling Analysis

The scaling analysis was first carried out using analytical expressions to estimate the stiffness and natural frequency of the boring bars as functions of Ø and *L*. The resulting trends, shown in Figure 5, highlight a clearly non-linear relationship between geometry and dynamic behavior. This confirms that the performance of large boring bars cannot be reliably extrapolated with linear scaling rules, emphasizing the relevance of the proposed methodology.

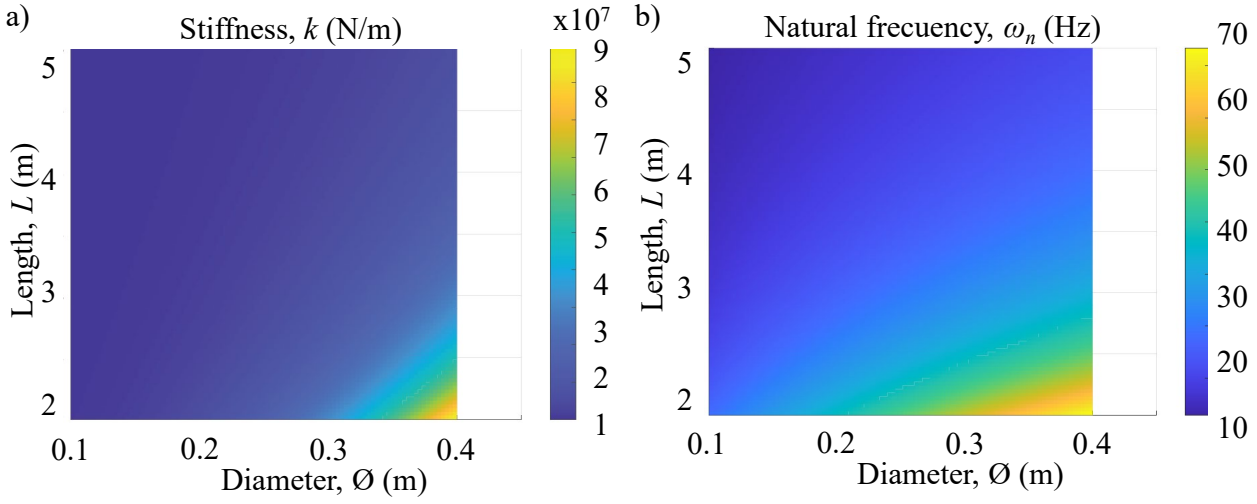

Fig. 5. Scalation analysis of boring bars in function of Ø and L: a) stiffness, and b) natural frequency.

The results reveal that both stiffness and the first bending frequency drop sharply when the diameter decreases or the length increases. Beyond a certain slenderness level, however, the response begins to flatten, indicating that once the bar becomes extremely slender, further geometric changes have a comparatively small influence on dynamics. In contrast, within the moderate-slenderness region, the steepest portion of the curves, even small geometric adjustments generate significant improvements in stiffness, offering a favorable window for internal design optimization for example.

The sensitivity study reinforces that diameter is the dominant parameter influencing dynamic behavior, producing far greater improvements than comparable adjustments in length. As a result, moderate increases in diameter consistently deliver a more substantial gain in stiffness and frequency than reducing the overhang.

Based on these findings, the 14×Ø scaling study was completed for the two target diameters bar (Ø200). It should be noted that if different length-to-diameter ratios are required, the scaling factors derived may not remain applicable.

3.2. TMD Design Tuning

The TMD was first tuned for case study boring bar following the stablished methodology. The process began with the selection and experimental characterization of the flexible couplings to determine their effective stiffness k_2. The couplings were tested under bending in the same direction as in the TMD assembly: the upper side was fixed, the lower side was connected to the TMD cap mounted on a dynamometer, and controlled displacements were applied using a machine-tool. The resulting reaction forces allowed quantification of the coupling stiffness, yielding $k_2 = 0.2$ N/µm.

With the coupling stiffness defined, the TMD mass (m_2) was determined using the tuning criterion that matches the absorber frequency to the natural frequency of the boring bar. Based on the modal parameters in Figure 6 ($\omega_1 = 22$ Hz), the boring bar required a 10 kg mass. The resulting mass ratios was approximately of 10%, valid for optimal dynamic attenuation. Achieving higher mass ratios would require stiffer couplings to allow larger masses without detuning, which were not available in this study. The simulated FRF with and without the TMD are shown in Figure 6. The TMD successfully reduces the original resonance peak, demonstrating effective energy extraction from the primary bending mode. The real part of the FRFs (Figure 6) further confirms these trends. The critical mode maximum peak and amplitude reduction closely match predictions.

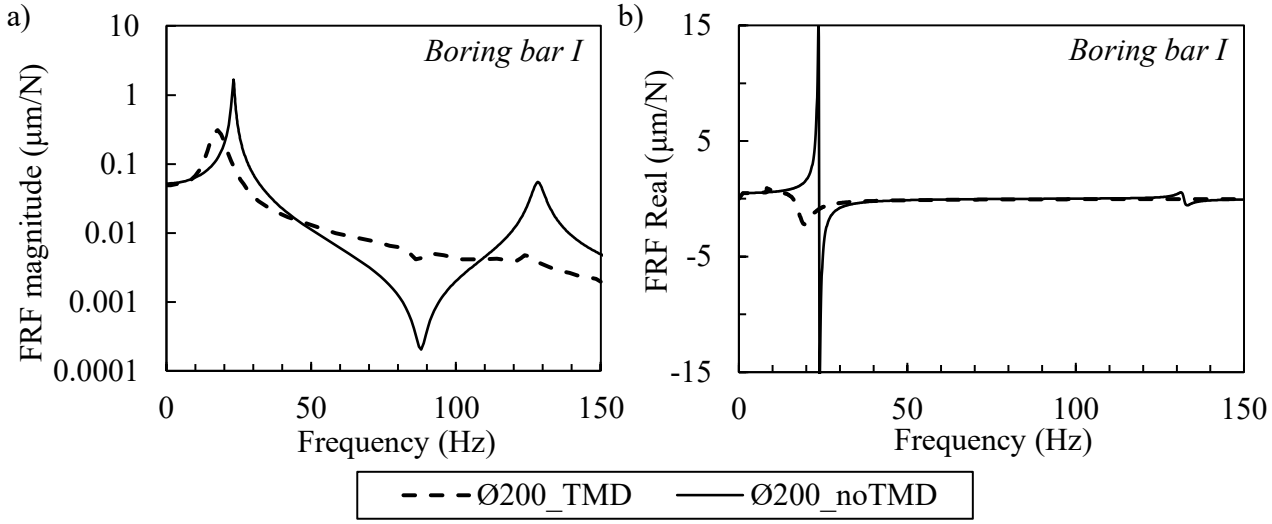

Fig. 6. Boring bar FRF with TMD vs noTMD for a) Magnitude of the FRF, and b) Real part of the FRF.

3.3. Experimental Validation

The prototype of the boring bar of Ø200 mm equipped with the TMD was tested experimentally at several overhang lengths (L'), ranging from the target configuration of 2800 mm (14×Ø) down to 1300 mm, in order to evaluate the dynamic behavior over a representative operating range. A comparison between the predicted and experimental FRFs at the largest overhang configuration shows that the experimentally measured natural frequency (Figure 7) was slightly lower than the predicted value (Figure 6) and exhibited higher damping, which is attributed primarily to the additional mass and higher attenuation introduced by the damping fluid and other TMD assembly components not explicitly represented in the analytical model. The frequency deviation remained

below 10%, and the reduced response magnitude indicates clear increase in actual damping, thereby confirming that the predictive models provide adequate accuracy for design and tuning purposes.

The experimental tests conducted across different overhang lengths revealed the expected increase in stiffness and natural frequency as the bar length decreased (Figure 7). As a result, shorter overhangs inherently exhibit significantly higher dynamic stiffness and reduced vibration amplitudes, even without considering the contribution of the TMD. For this reason, it is essential to distinguish between two effects observed in Figure 7; first, the structural stiffening effect caused by shortening the overhang, which shifts the natural frequency to higher values and inherently reduces the FRF magnitude; and second, the vibration attenuation effect produced by the TMD, which is most effective when the excitation frequency coincides with the tuned natural frequency at 14×Ø configuration.

The reduced FRF magnitude at shorter overhang lengths is primarily due to increased structural stiffness rather than improved TMD performance. Since the absorber was tuned to the natural frequency of the 14×Ø configuration, its effectiveness decreases as the bar stiffens and the natural frequency shifts, leading to detuning and reduced damping capability. Although shorter overhangs would typically be machined using different boring bars in industrial settings, these results provide valuable insight into how bar length affects dynamic behavior and TMD performance in large tools. Specifically, the results demonstrate that optimal TMD performance in large-scale boring applications requires tuning to the dominant bending mode corresponding to the intended overhang length.

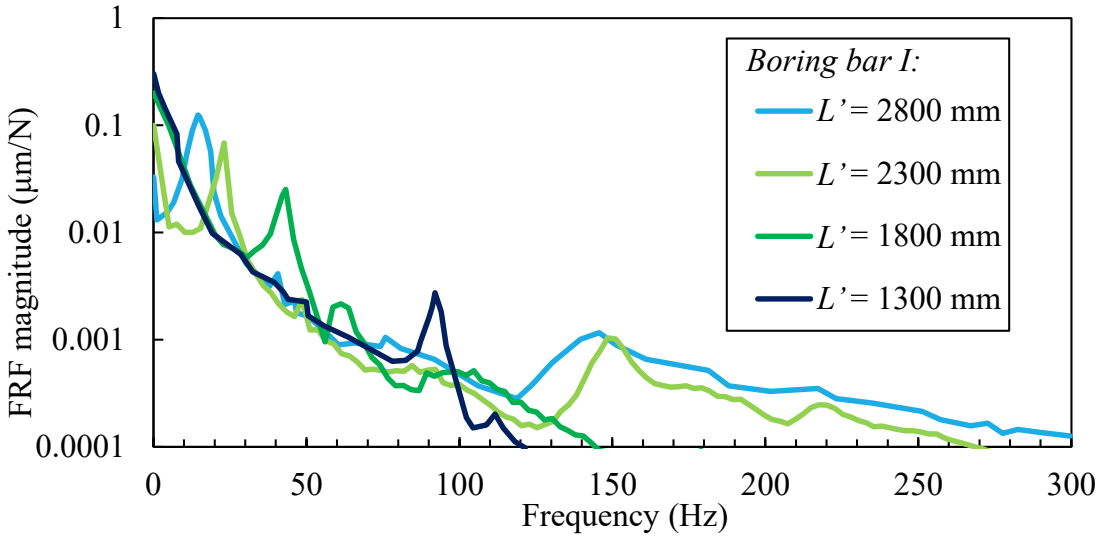

Fig. 7. Experimental FRF results across the different lengths (L') with the boring bar of Ø200.

4. Conclusion

A scaling methodology for the development of large boring bars with integrated TMDs has been presented and validated. The approach was applied and experimentally validated on a boring bar with a diameter of Ø200 mm and a length-to-diameter ratio of 14×Ø. The main findings are:

- The scaling analysis confirms that the external diameter is the dominant parameter governing the dynamic behavior of large boring bars. For tools sharing the same diameter-to-length ratio, geometry can be reliably scaled using the identified factors. However, TMD tuning does not follow a linear scaling law: it depends strongly on the stiffness of the flexible couplings, requiring diameter-specific tuning to maintain optimal vibration attenuation.
- The proposed methodology provides a structured framework for optimizing boring bar design and integrating TMDs suitable for large tool geometries. The resulting TMD configuration demonstrates clear advantages when scaled to large boring bars, offering substantial improvements in dynamic performance while maintaining an efficient and practical design approach.

- Experimental validation confirms the effectiveness of the methodology. The Ø200 mm prototype exhibited clear vibration attenuation at the target overhang, demonstrating that the TMD was correctly tuned for the intended operating length. Additional tests performed at shorter overhangs confirmed the expected variation in dynamic behavior and provided insight into the usable operating range of the boring bar.

Acknowledgement

The authors hereby thank the financial support from the TAILORSURF (PID2022-139655OB-I00), ORLEGI (KK-2024/00005), and MAND (ZL-2023/00856) projects, as well as the Basque Government for the predoctoral grant (PRE_2023_1_0134) and the research group support: Grupo de Excelencia A (IT1443-22).

References

[1] K. J. Kaliński, M. A. Galewski, M. R. Mazur, and N. Stawicka-Morawska, "An improved method of minimizing tool vibration during boring holes in large-size structures," *Materials*, vol. 14, no. 16, Aug. 2021, doi: 10.3390/ma14164491.

[2] Khramov, I. Semdyankin, and E. Kiselev, "Improving the performance of the processing of deep holes by improving the structure of the boring tool," in *IOP Conference Series: Materials Science and Engineering*, Institute of Physics Publishing, Jan. 2020. doi: 10.1088/1757-899X/709/4/044068.

[3] Y. Altintas, G. Stepan, E. Budak, T. Schmitz, and Z. M. Kilic, "Chatter stability of machining operations," *J Manuf Sci Eng*, vol. 142, no. 11, 2020.

[4] G. Quintana and J. Ciurana, "Chatter in machining processes: A review," May 2011. doi: 10.1016/j.ijmachtools.2011.01.001.

[5] J. Munoa *et al.*, "Chatter suppression techniques in metal cutting," *CIRP Annals*, vol. 65, no. 2, pp. 785–808, 2016, doi: 10.1016/j.cirp.2016.06.004.

[6] W. Thomas, J. Peterka, T. Szabó, M. V. Albuquerque, R. Pederiva, and L. P. Kiss, "Analytical and Experimental Investigation of the Dynamic Stability in Passive Damper Boring Bars," in *Procedia CIRP*, Elsevier B.V., 2023, pp. 187–192. doi: 10.1016/j.procir.2023.03.033.

[7] Sandvik Coromant, "CoroBore Lightweight." Accessed: Sep. 30, 2022. [Online]. Available: https://www.sandvik.coromant.com/en-us/products/corobore-lightweight/pages/default.aspx.

[8] Tony L. Schmitz and K. Scott Smith, "Machining Dynamics Frequency Response to Improved Productivity Second Edition," 2019. doi: https://doi.org/10.1007/978-3-319-93707-6.

[9] J. Munoa, A. Iglesias, A. Olarra, Z. Dombovari, M. Zatarain, and G. Stepan, "Design of Modular Damped Fixturing System by Means of Self-Tuneable Mass Damper," *CIRP Annals*, vol. 65, no. 1, 2016.

[10] J. Munoa, A. Iglesias, A. Olarra, Z. Dombovari, M. Zatarain, and G. Stepan, "Design of self-tuneable mass damper for modular fixturing systems," *CIRP Annals*, vol. 65, no. 1, pp. 389–392, 2016, doi: https://doi.org/10.1016/j.cirp.2016.04.112.

[11] G. Aguirre, M. Gorostiaga, T. Porchez, and J. Muñoa, "Self-tuning semi-active tuned-mass damper for machine tool chatter suppression," *ISMA2012-USD2012*, vol. 1, pp. 109–123, 2012.

[12] Y. Nakano, T. Kishi, and H. Takahara, "Experimental study on application of tuned mass dampers for chatter in turning of a thin-walled cylinder," *Applied Sciences (Switzerland)*, vol. 11, no. 24, Dec. 2021, doi: 10.3390/app112412070.

[13] R. Kishore, S. K. Choudhury, and K. Orra, “On-line control of machine tool vibration in turning operation using electro-magneto rheological damper,” *J Manuf Process*, vol. 31, pp. 187–198, Jan. 2018, doi: 10.1016/j.jmapro.2017.11.015.

[14] L. Liu, Y. Xu, F. Zhou, G. Hu, and L. Yu, “Performance Analysis of Magnetorheological Damper with Folded Resistance Gaps and Bending Magnetic Circuit,” *Actuators*, vol. 11, no. 6, Jun. 2022, doi: 10.3390/act11060165.

[15] D. Mei, Z. Yao, T. Kong, and Z. Chen, “Parameter optimization of time-varying stiffness method for chatter suppression based on magnetorheological fluid-controlled boring bar,” *International Journal of Advanced Manufacturing Technology*, vol. 46, no. 9–12, pp. 1071–1083, Feb. 2010, doi: 10.1007/s00170-009-2166-9.

[16] D. S. Pour and S. Behbahani, “Semi-active fuzzy control of machine tool chatter vibration using smart MR dampers,” *International Journal of Advanced Manufacturing Technology*, vol. 83, no. 1–4, pp. 421–428, Mar. 2016, doi: 10.1007/s00170-015-7503-6.

[17] J. Albizuri, M. H. Fernandes, I. Garitaonandia, X. Sabalza, R. Uribe-Etxeberria, and J. M. Hernández, “An active system of reduction of vibrations in a centerless grinding machine using piezoelectric actuators,” *Int J Mach Tools Manuf*, vol. 47, no. 10, pp. 1607–1614, Aug. 2007, doi: 10.1016/j.ijmachtools.2006.11.004.

[18] A. Matsubara, M. Maeda, and I. Yamaji, “Vibration suppression of boring bar by piezoelectric actuators and LR circuit,” *CIRP Ann Manuf Technol*, vol. 63, no. 1, pp. 373–376, 2014, doi: 10.1016/j.cirp.2014.03.132.

[19] J. Lin, J. Han, M. Lu, B. Yu, and Y. Gu, “Design, analysis and testing of a new piezoelectric tool actuator for elliptical vibration turning,” *Smart Mater Struct*, vol. 26, no. 8, Aug. 2017, doi: 10.1088/1361-665X/aa71f0.

[20] F. Chen, X. Lu, and Y. Altintas, “A novel magnetic actuator design for active damping of machining tools,” *Int J Mach Tools Manuf*, vol. 85, pp. 58–69, 2014, doi: 10.1016/j.ijmachtools.2014.05.004.

[21] F. Chen and G. Liu, “Active damping of machine tool vibrations and cutting force measurement with a magnetic actuator,” *International Journal of Advanced Manufacturing Technology*, vol. 89, no. 1–4, pp. 691–700, Mar. 2017, doi: 10.1007/s00170-016-9118-y.

[22] S. Wan, X. Li, W. Su, J. Yuan, J. Hong, and X. Jin, “Active damping of milling chatter vibration via a novel spindle system with an integrated electromagnetic actuator,” *Precis Eng*, vol. 57, pp. 203–210, May 2019, doi: 10.1016/j.precisioneng.2019.04.007.

[23] D. Tomasoni, L. Giorleo, and E. Ceretti, “Milling tool optimization by topology optimization technique,” in *ESAFORM 2021 - 24th International Conference on Material Forming*, PoPuPS (University of LiFge Library), 2021. doi: 10.25518/esaform21.3972.

[24] P. Hanzl, M. Zetek, V. Rulc, H. Purs, and I. Zetkova, “Finite Element Analysis of a Lightweight Milling Cutter for Metal Additive Manufacturing,” *Manufacturing Technology*, 2020.

[25] M. Etxebeste, G. Ortiz-de-Zarate, I. M. Arrieta, and P. J. Arrazola, “A virtual design methodology to improve the dynamics and productivity of large milling tools,” *J Manuf Process*, vol. 134, pp. 1096–1113, Jan. 2025, doi: 10.1016/j.jmapro.2025.01.024.

[26] J. Do Suh and D. Lee, “Design and manufacture of hybrid polymer concrete bed for high-speed CNC milling machine,” *International Journal of Mechanics and Materials in Design*, vol. 4, pp. 113–121, Jun. 2008, doi: 10.1007/s10999-007-9033-3.

[27] J.-H. Kim and S.-H. Chang, “Design of μ-CNC machining centre with carbon/epoxy composite–aluminium hybrid structures containing friction layers for high damping capacity,” *Compos Struct*, vol. 92, no. 9, pp. 2128–2136, 2010.

[28] M. Kim, J. H. Kim, M. Lee, and S. K. Lee, "Surface finish improvement using a damping-alloy sleeve-insert tool holder in the end milling process," *International Journal of Advanced Manufacturing Technology*, vol. 106, no. 5–6, pp. 2433–2449, Jan. 2020, doi: 10.1007/s00170-019-04757-0.

[29] E. Abele, M. Haydn, and T. Grosch, "Adaptronic approach for modular long projecting boring tools," *CIRP Ann Manuf Technol*, vol. 65, no. 1, pp. 393–396, 2016, doi: 10.1016/j.cirp.2016.04.104.

[30] B.-K. Min, G. O'neal, Y. Koren, and Z. Pasek, "A smart boring tool for process control."

[31] L. Rubio, J. A. Loya, M. H. Miguélez, and J. Fernández-Sáez, "Optimization of passive vibration absorbers to reduce chatter in boring," *Mech Syst Signal Process*, vol. 41, no. 1–2, pp. 691–704, Dec. 2013, doi: 10.1016/j.ymssp.2013.07.019.

[32] E. Marui, S. Ema, M. Hashimoto, and Y. Wakasawa, "Plate insertion as a means to improve the damping capacity of a cutting tool system," 1998.

[33] S. Ema and E. Marui, "Suppression of chatter vibration of boring tools using impact dampers," *Int J Mach Tools Manuf*, vol. 40, 2000.

[34] R. S. Hahn, "Design of Lanchester Damper for Elimination of Metal-Cutting Chatter," *Transactions of the American Society of Mechanical Engineers*, vol. 73, no. 3, pp. 331–335, Jul. 2022, doi: 10.1115/1.4016247.

[35] Y. H. J. Au, K. W. Ng, and R. W. New, "The Lanchester Damper—A Design Procedure for Optimizing the Damping Ratio for a Cylindrical Slug Damper Fitted to a Machine Element," 1979.

[36] Y. Yang, D. Xu, and Q. Liu, "Milling vibration attenuation by eddy current damping," *The International Journal of Advanced Manufacturing Technology*, vol. 81, pp. 445–454, 2015.

[37] W. S. Yip and S. To, "Reduction of tool tip vibration in single-point diamond turning using an eddy current damping effect," *The International Journal of Advanced Manufacturing Technology*, vol. 103, pp. 1799–1809, 2019.

[38] Sandvik Coromant, "Silent Tools for turning." *https://www.sandvik.coromant.com/es-es/tools/turning-tools/internal-turning-tools/silent-tools-turning*.

[39] M. Etxebeste, G. Ortiz-De-Zarate, I. M. Arrieta, and P. J. Arrazola, "Finite Element Modeling to Design Optimized TMD for Milling Tools," in *Procedia CIRP*, Elsevier B.V., 2025, pp. 448–453. doi: 10.1016/j.procir.2025.02.077.

[40] W. Hintze, M. Hinrichs, O. Rosenthal, U. Schleinkofer, and R. Venturini, "Model based design of tuned mass dampers for boring bars of small diameter," *Procedia CIRP*, vol. 117, pp. 193–198, 2023, doi: https://doi.org/10.1016/j.procir.2023.03.034.

[41] S. Ghorbani, V. A. Rogov, A. Carluccio, and P. S. Belov, "The effect of composite boring bars on vibration in machining process," *International Journal of Advanced Manufacturing Technology*, vol. 105, no. 1–4, pp. 1157–1174, Nov. 2019, doi: 10.1007/s00170-019-04298-6.

[42] Y. Alammari, M. Sanati, T. Freiheit, and S. S. Park, "Investigation of Boring Bar Dynamics for Chatter Suppression," in *Procedia Manufacturing*, Elsevier B.V., 2015, pp. 768–778. doi: 10.1016/j.promfg.2015.09.059.

[43] FAT HACO, "Machining technologies in lathes from FAT HACO ," 2025.

[44] J. Tlusty, "The stability of the machine tool against self-excited vibration in machining," *Proc. Int. Res. in Production Engineering, Pittsburgh, ASME*, vol. 465, 1963.

The publication of this article was funded by the Mondragon Goi Eskola Politeknikoa, J.M.A. S.Coop